Coupled DC-SQUID Dynamics

Lacerda Santos Neto Antonio,

I. Introduction

Current biased dc superconducting quantum interference devices (SQUIDs) are composed of two Josephson junctions connected by a superconducting loop. These devices have been extensively employed as magnetic sensors [6] and as building blocks for quantum circuits [4]. Additionally, they show good results when used as superconducting phase qubits [8].

In the latter application, the quantized variation of the voltage between one of the Josephson junctions forming the SQUID as a function of the superconducting phase difference across the junction (the "washboard potential" see [5, 3]) is used to form the $|0\rangle$ and $|1\rangle$ states of the qubit [3, 5]. In fact, depending on the parameters of the SQUID, one of the potential dips in the washboard potential can be used as a potential well centred around a given phase. The occupancy of the sates in the potential well can then be modulated by external factors, such as a magnetic field going through the SQUID [3, 5].

Considering that the quality of a qubit is related, among other factors, to its stability over time isolated from external factors or under the influence of, e.g. and electromagnetic field, studying the dynamics of such system is of considerable interest. Moreover, from the previous paragraph one can see that one important parameter in such a system is the phase across each Josephson junction. In fact, for SQUIDs, where the phase of each junction is coupled to each other, the relevant parameter is the difference (x) and sum (y) of the two phases. Therefore, in this article, the dynamics of the SQUID with regard to x and y is studied. In part II the model and the equations of motion for x an y will be deduced and in part III the fixed points and their stability will be studied as a function of ; i) the coupling intensity between the two junctions, ii) the applied magnetic field and iii) the bias current.

II. Physical model of a dc-SQUID qubit

Following Mitra et.al [4] the dc-SQUID is modelled here by the circuit shown in Fig.1. There one can see the two Josephson junctions J_1, J_2 with a junction capacitance C_1 and C_2 each. The two sides of the superconducting loop are assumed to have an inductance L_1 and L_2. I is the current applied to the SQUID and Φ_a the flux going through the superconducting loop. The latter is generated by I_f going through the mutual inductance M. The resistance is neglected as long as $I < I_c$, with I the current going through J_1 and J_2 and I_c the junction critical current, assumed the same for both junctions. Therefore, the two parameters allowing for the control of the qubit is Φ_a and I.

This circuit can be described by the Lagrangian :

$$\mathrm{L}(\gamma_1, \dot{\gamma}_1, \gamma_2, \dot{\gamma}_2) = \frac{m_1 \dot{\gamma_1}^2}{2} + \frac{m_2 \dot{\gamma_2}^2}{2} - U(\gamma_1, \gamma_2) \qquad (1)$$

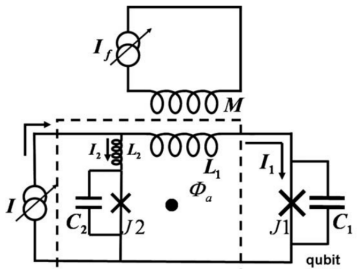

Fig. 1. Circuit used to model the dc-SQUID qubit. The two Josephson junctions are J_1, J_2 and they have a junction capacitance C_1 and C_2. The two sides of the SQUID are assumed to have an inductance L_1 and L_2. I is the current applied to the SQUID and Φ_a the flux going through the superconducting loop. The latter is generated by I_f going through the mutual inductance M [4].

where $m_i = \frac{\Phi_0}{2\pi}^2 C_i$, with $\Phi_0 = \frac{h}{2e}$ as the flux quantum, γ_1 and γ_2 the phase across the junctions J_1 and J_2 and $U(\gamma_1, \gamma_2)$ is a potential defined as :

$$U(\gamma_1, \gamma_2) = -E_{J1}\cos(\gamma_1) - \frac{\Phi_0 L_2 I \gamma_1}{2\pi L} - E_{J2}\cos(\gamma_2) - \frac{\Phi_0 L_2 I \gamma_2}{2\pi L} + (\frac{\Phi_0}{2\pi})^2 \frac{1}{2L}\left(\gamma_1 - \gamma_2 - 2\pi\frac{\Phi_a}{\Phi_o}\right)^2 \qquad (2)$$

where $E_{Ji} = I_c \frac{\Phi_0}{2\pi}$ the Josephson energy, with I_c the critical current, and $L = L_1 + L_2$. From Eq.1 and Eq.2 one can then deduce[1] that the equation of motion for γ_1 is [4] :

$$\frac{\Phi_0}{2\pi} C_1 \ddot{\gamma_1} + I_c \sin(\gamma_1) = I\frac{L_2}{L} - \frac{\Phi_0}{2\pi L}\left(\gamma_1 - \gamma_2 - 2\pi\frac{\Phi_a}{\Phi_0}\right) \qquad (3)$$

The equation above (Eq.3) does not take into account loss in the system. It is nonetheless noticeable the resemblance of the latter with the one obtained by applying the Resistvely Shunted Junction (RSJ) model [7, 3] (which has been used by [2, 1]), i.e. :

$$\ddot{\gamma_1} + \beta\dot{\gamma_1} + \sin(\gamma_1) + i_F(t) = i* \qquad (4)$$

with β a loss term, $i* \equiv I/I_c$, and $i_F(t)$ represents white noise, which will be considered constant and thus taken into account by $i*$. One can notice here that the biggest difference between Eq.3 and Eq.4 is the superconducting phase coupling term, necessary when studying a SQUID, and the loss term, which was not taken into account due to the use of the Lagrangian. From now on, $\beta\dot{\gamma_1}$ will be added to Eq.3 in order to provide a more realistic system of equations. Therefore,

[1] Here only the Euler relation, current conservation and the flux phase relation for the SQUID loop are used. No assumption concerning the parameters is made. See Mitra et.al for a more detailed discussion

one obtains the system (the second equation is obtained by replacing 1 with 2 and 2 with 1) :

$$\frac{\Phi_0}{2\pi}C_1\ddot{\gamma_1} + \beta\dot{\gamma_1}I_c\sin(\gamma_1) = I\frac{L_2}{L} - \frac{\Phi_0}{2\pi L}\left(\gamma_1 - \gamma_2 - 2\pi\frac{\Phi_a}{\Phi_0}\right) \tag{5}$$

In order to obtain a dimensionless system of equations, the following change of variables is used : $i = I/2I_c$, $\phi = \Phi_a/\Phi_0$, $\alpha = \Phi_0/(I_cL2\pi)$, $\Omega_1 = \sqrt{I_c2\pi/C_1\Phi_0}$, $l_2 = L_2/L$, $\tau_1 = \Omega_1 t$ and $\varepsilon = \beta 2\Omega/I_c$. Therefore, Eq.5 becomes :

$$\ddot{\gamma_1} + \varepsilon\dot{\gamma_1} + \sin(\gamma_1) = il_2 + \alpha 2\pi\phi - \alpha(\gamma_1 - \gamma_2) \tag{6}$$

Here the indices for ε and τ are dropped since $C_1 = C_2$ is assumed. Moreover, from now on $\dot{\gamma}$ is defined as $\frac{d\gamma}{d\tau}$. Finally, in order to study this system the variables $x = \frac{(\gamma_1-\gamma_2)}{2}$ and $y = \frac{(\gamma_1+\gamma_2)}{2}$ are introduced. The following system of equations is found :

$$\begin{aligned}
\dot{x} &= u \\
\dot{y} &= v \\
\ddot{x} &= 2\pi\alpha\phi - \frac{i(l_2-l_1)}{2} - \varepsilon u - 2\alpha x - \sin(x)\cos(y) \\
\ddot{y} &= -\varepsilon v + \frac{i}{2} - \sin(y)\cos(x)
\end{aligned} \tag{7}$$

Where α is the coupling coefficient, ε is the loss coefficient and assumed to be positive, ϕ represents the flux and i the current going through the SQUID. Concerning the parameter i it is always smaller than 2 since the current going through the junction must be smaller than I_c if the superconducting behaviour is to be maintained. It is worth to notice though that $i = 2$ is only possible if : i) the impedance due to $C_{1,2}$ is the same as the one for $J_{1,2}$; ii) one has two identical Josephson junctions and iii) $l_1 = l_2$. The later is highly unlikely, moreover, near I_c the superconducting properties begin to degrade, thus, $|i| < 0.5$ is a realistic limit. Finally, $\phi > 0$ and ε is set to 0.15, which was the value used by [2].

III. Fixed Points and stability

Firstly, one can see that Eq.6 is invariant under the transformation $\gamma_{1,2} \to \gamma_{1,2}+2\pi$, $\gamma_{2,1} \to \gamma_{1,2}$ and $(\gamma_i, i) \to (-\gamma_i, -I)$. The same is valid for Eq.7. One can thus consider $i \geq 0$.

From Eq.7 one can see that the fixed points will be $(x_0, y_0, 0, 0)$, with :

$$\begin{cases} \sin x_0\left(1 - \dfrac{i^2}{4\cos {x_0}^2}\right)^{1/2} = 2\pi\alpha\phi - \dfrac{i(l_2-l_1)}{2} - 2\alpha x_0 \\ y_0 = \arcsin\dfrac{i}{2\cos x_0} \end{cases} \tag{8}$$

$$\begin{cases} \cos y_0\left(1 - \dfrac{i^2}{4\sin {y_O}^2}\right)^{1/2} = 2\pi\alpha\phi - \dfrac{i(l_2-l_1)}{2} \\ \qquad\qquad -2\alpha\arccos\dfrac{i}{2\sin y_0} \\ x_0 = \arccos\dfrac{i}{2\sin y_0} \end{cases} \tag{9}$$

In order to study the stability for each fixed point, the eigenvalues of the Jacobian defined in Eq.10 must be calculated :

$$J = \begin{bmatrix} 0 & 0 & 1 & 0 \\ 0 & 0 & 0 & 1 \\ -(\cos x\cos y + 2\alpha) & \sin x\sin y & -\varepsilon & 0 \\ \sin x\sin y & -\cos x\cos y & 0 & -\varepsilon \end{bmatrix} \tag{10}$$

One must thus solve the quadratic equations bellow to find the eingevalues of Eq.10.

$$\begin{cases} \lambda^2 + \varepsilon - E_{1,2} = 0 \\ E_{1,2} = \frac{1}{2}\left(tr(E) \pm \sqrt{tr(E)^2 - 4det(E)}\right) \end{cases} \tag{11}$$

With the matrix E defined as :

$$E = \begin{bmatrix} -(\cos x\cos y + 2\alpha) & \sin x\sin y \\ \sin x\sin y & -\cos x\cos y \end{bmatrix} \tag{12}$$

From Eq.8 and Eq.9 we can see that there might be fixed points only if : i) $|cos(x_0)| > i/2$ and $(-\frac{i(l_2-l_1}{2} + 2\pi\alpha - 1) < 2\alpha x_0 < (-\frac{i(l_2-l_1}{2} + 2\pi\alpha + 1)$, $\forall y$ or ii) $|sin(y_0)| > i/2$ and $-2\pi\alpha\phi + \frac{i(l_2-l_1)}{2} - 1 < 2\alpha\arccos\frac{i}{2\sin y_0} < -2\pi\alpha\phi + \frac{i(l_2-l_1)}{2} + 1$, $\forall x$.

Concerning the stability of each fixed point, it depends on the sign of $E_{1,2}$. Here one can have : i) $E_{1,2} < 0$, in which case the point will be stable (since $\varepsilon > 0$), with oscillatory terms appearing in the general solution if $\varepsilon^2 < 4|E_{1,2}|$ and a center appearing if $\varepsilon = 0$, i.e. if there is no loss; ii) $E_{1,2} > 0$, which will lead to a $2D$ stable manifold an $2D$ unstable manifold; iii) $E_1 > 0$ and $E_2 < 0$, in which case one will have an $1D$ unstable manifold and a $3D$ stable manifold, with an oscillatory behaviour along 2 dimensions if $\varepsilon^2 < 4|E_2|$.

A. Uncoupled Josephson junctions under no magnetic field

In case the junctions are not coupled, there is no magnetic field being applied and $l_1 = l_2$, the conditions defining the fixed points are reduced to :

$$\begin{cases} x_0 = n\pi \quad \text{for} \quad n \in \mathbf{N} \\ y_0 = (-1)^n \arcsin\frac{i}{2} \end{cases} \tag{13}$$

$$\begin{cases} y_0 = \dfrac{2m+1}{2}\pi \quad \text{for} \quad m \in \mathbf{N} \\ x_0 = (-1)^m \arccos\frac{i}{2} \end{cases} \tag{14}$$

Considering that the solutions are 2π periodic (c.f Sec.III), it is enough to study the stability around the fixed point for $n, m = 0, 1$ in order to obtain a qualitative assessment of the system.

For $n = 0$, the fixed point is $(0, \arcsin(i/2), 0, 0)$, which means that $E_{1,2} < 0$ and the fixed point is stable. Considering that, from the definition of x an y, $(0, \arcsin(i/2), 0, 0)$ implies that $\gamma_1 = \gamma_2$ and $\gamma_1 + \gamma_2 \leq \pi$, $\gamma_1, \gamma_2 \in [0, \pi/2]$. Therefore, for $\gamma_1, \gamma_2 \in [0, \pi/2]$ and $\varepsilon > 0$, the solution will be stable. For $n = 1$ the fixed point is $(\pi, \pi/2 - \arccos(i/2), 0, 0)$

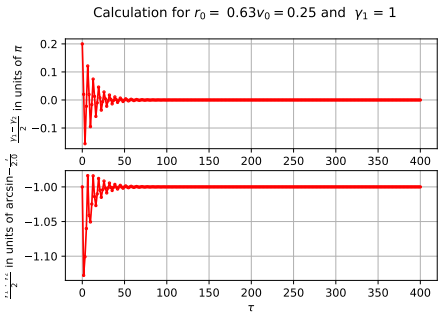

Fig. 2. Numerical calculation of the time dependence of the system described by Eq.7 near a stable fixed point.

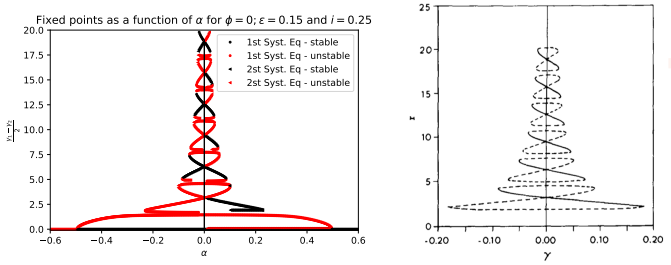

Fig. 3. On the left the first six families of the fixed points for the system of equations in 7 is shown. They were obtained by solving 8 and 9. On the right the results obtained by Doedel et al. [2].

and $E_{1,2} < 0$, thus for $\gamma_1, \gamma_2 \in [\pi/2, \pi]$ and $\varepsilon > 0$, the solution will have a $2D$ stable manifold an $2D$ unstable manifold. Finally, for $m = 0, 1$, $E_1 < 0$ and $E_2 > 0$ with $\gamma_1 \in [0, \pi/2]$ and $\gamma_2 \in [\pi/2, \pi]$. Therefore, these solutions have a $1D$ unstable manifold and a $3D$ stable manifold, with an oscillatory behaviour along 2 dimensions if $\varepsilon^2 < 4\,|E_2|$.

In order to study the time dependence of x and y one can numerically calculate Eq.7. Therefore, for $\varepsilon = 0.15$, $i = 0.5$, $l_1 = l_2 = 0.5$ and $\phi = \alpha = 0$, Fig.III-A shows the time dependence for x and y in function of the initial conditions ($x = r_0$ and $y = v_0$). One can thus see that the system does indeed converge towards $(0, \arcsin(i/2), 0, 0)$ for Fig.III-A.

B. Coupled Josephson junctions under no magnetic field

In a DC-SQUID the two Josephson junctions are coupled to each other. This is represented by a non zero α term in Eq.7. It is thus interesting to study how the system evolves as α changes. In order to do so, the inductance in each side of the squid loop was assumed identical ($l_1 = l_2$), i was set to 0.25, ε to 0.15 and $\phi = 0$. The system of equations 8 and 9 were solved graphically and the Jacobian 10 diagonalized with a python script [2].

In Fig.III-B one can see the variation of x_0 with γ. Th results in black correspond to stable fixed points and in red unstable fixed points. Here $\alpha \in [-0.7, 0.7]$.

The Fig.III-B shows that as γ increases, the distance between two fixed points will decrease until they collapse into each other. This is the characteristic behaviour of saddle-node

[2] One can have access to it by going to https://github.com/asantosnet/SD_SQUID

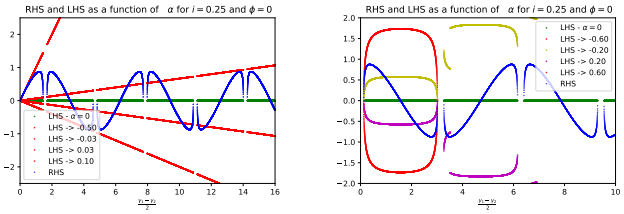

Fig. 4. On the left, in blue is shown the RHS of the first equation in 8 as a function of x and the LHS is shown in red and green for different values of α. Their crossings correspond to fixed points. On the right the RHS and LHS of the first equation in 9 is shown.

bifurcations. Therefore, the total number of fixed points decreases as γ increases by a series of saddle-node bifurcations. More precisely, for a sufficiently large γ there will be no solution respecting 9 and there will only be one solution for 8. Indeed, by plotting the left hand side (LHS) and the right hand side (RHS) of the first equation in 8 (see Fig.III-B), one sees that they will only intersect at a point different than $x_0 = 0$ as long as $-0.5 \leq \alpha \leq 0.10$.

The Fig.III-B is the result obtained by Doede et.al [2] and shows the first six families of fixed points. It shows that each family of fixed points has four rest points, among them one stable, and, as discussed, a finite number of fixed points for $\alpha \neq 0$ that decreases by saddle node bifurcation with increasing α. Moreover, each fixed point in one family is equivalent mod 2π to another fixed point in any of the existing families of the system. Moreover, by comparing the latter with Fig.III-B, the fixed points obtained with the first set of equations (8) seems to have the same stability, nonetheless, for the ones obtained with 9, that is not the case. This lack of agreement with the literature is very likely due to an issue in the python script used and it seems to originate from a problem when taking into consideration the periodicity of the $\arcsin$ and $\arccos$ functions.

Finally, Fig.III-B and to a certain extent Fig.III-B shows that after applying an external stimuli, such as a magnetic field, the system should converge towards a stable point with $\gamma_1 \neq \gamma_2$ even for two coupled Josephson junctions as long as the coupling in the latter is not too large and the the phase difference between the junctions x is bigger than a minimum value that can be determined from Fig.III-B.

C. Coupled Josephson junctions under magnetic field and bias current

In order to study the effect of ϕ and i on the behaviour of the SQUID, ε is set to 0.15, l_1 and l_2 are the same and $\alpha = 0.05$.

The fixed points obtained as a function of the current i and for a $\phi = 2$ is shown in Fig.III-C. Although the image is noisy and not "periodic" , likely due to the error described in the previous section, it is possible to notice a certain pattern which indicates that, as i increases, the fixed points come, two by two, closer to each other and cease to exist after a saddle-node bifurcation. Moreover, Fig.III-C indicates as well that a current higher than ≈ 1 does not have a fixed point near $x = 0$, which could lead to a dephasing of the two junctions.

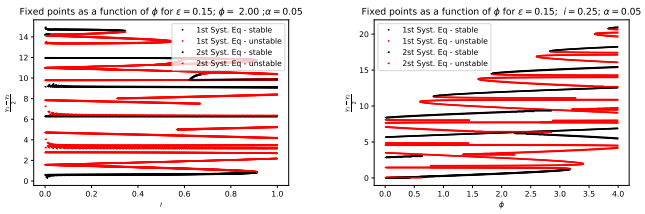

Fig. 5. Fixed points obtained solving the Jacobian 10 as a function of the current (on the left) and ϕ (on the right).

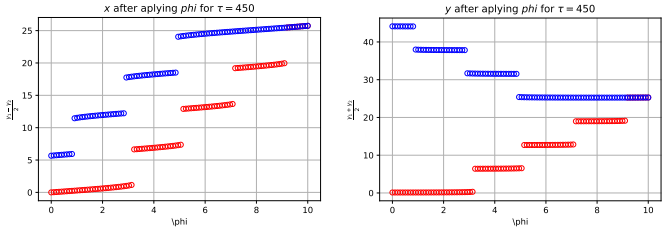

Fig. 6. Numerical calculation of the time dependence of the system under an applied magnetic field using the system of equations shown in 7. The variation of x and y are shown respectively on the left and on the Right. The red dots corresponds an increasing ϕ whereas the blue ones are calculations performed when ϕ was decreasing.

In the Fig.III-C the fixed points found as a function of the magnetic field ϕ are shown for $i = 0.25$. It is possible to see that the number of fixed points decreases with decreasing ϕ by a series of saddle-node bifurcations.

In order to obtain a better understating of this behaviour, it is necessary to study the time evolution of the system after a magnetic field ϕ is applied. Using the same python script employed in Sec.III-A to solve the differential equations in 7[3]. , the state of the system after applying a constant magnetic field is shown in Fig.III-C. The field was applied in steps of 0.1 and at each the step the field was maintained constant for $\tau = 450$. Moreover, $i = 0.25$, $l_1 = l_2 = 0.5$, $\alpha = 0.05$ and $\varepsilon = 0.05$.

Fig.III-C shows a quantization of the x and y values as a function of ϕ . When the magnetic field applied is suddenly set to zero, the phase difference x between the junctions will oscillate and tend to zero. This is show in Fig.III-C. Moreover, the velocity at which the decoherence will be lost increases with ε and should also be strongly dependent on the coupling coefficient. Interestingly, the sum of the phases of each Josephson junction will not tend to zero, but will start from zero and then diverge.

In case the field is slowly decreased (at the same ratio it was increased), the difference between the superconducting phase of each junction will no tend to zero, but to a value slightly higher than 5, which could correspond to a stable fixed point in the second group shown in FigIII-B. Therefore, by slowly increasing and then decreasing the magnetic field one could change the properties of the phase quibit. Finally, concerning the sum of the phases, it doubles in value.

[3] One can have access to it by going to https://github.com/asantosnet/SD_SQUID

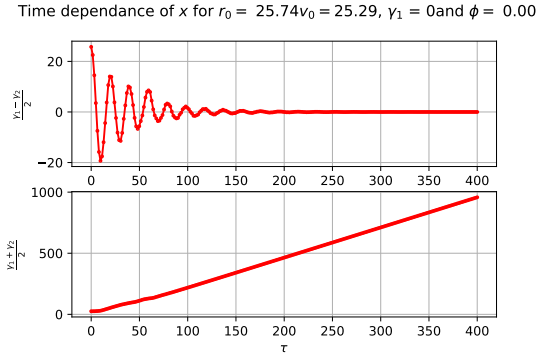

Fig. 7. Numerical calculation of the time dependence of the system when the magnetic field is suddenly set to zero after being kept at $\phi = 10$ for $\tau = 450$. 7.

IV. Conclusion

In this report the classical dynamics of the coupled DC-SQUID was studied. It has been shown that contrary to the uncoupled scenario, there is not an infinity of fixed points, but a finite number that decreases with increase coupling parameter by means of saddle-node bifurcations. A very similar behaviour might take place when increasing the current trough the SQUID and the opposite phenomena happens with the applied magnetic field, where the number of fixed nodes seems to increase as ϕ increases. Unfortunately, due to a problem in the program used to study the analytically solutions, the magnetic field and current effects on the stability and number of fixed points cannot be properly assessed. Concerning the evolution of the system with time τ, it has been shown that it might be possible to use an external magnetic field to change the difference between the superconducting phase of the Josephson junctions. Moreover, it was shown that if the field is decreased slowly with time, the changes might be, to a certain extent, conserved when the field is fully removed. Finally, it is important to notice that a high loss will rapidly attenuate the effect of the magnetic field on the phase difference once the latter is removed.

References

[1] D. G.; Doedel et al. In: *International Journal of Bifurcation and Chaos* 01 (01 Mar. 1991). DOI: 10.1142/s0218127491000051.

[2] E. J. Doedel et al. In: 35.7 (1988), pp. 810–817. ISSN: 0098-4094. DOI: 10.1109/31.1827.

[3] James A. Blackburn et al. In: *Physics Reports* (Nov. 2015). DOI: 10.1016/j.physrep.2015.10.010.

[4] Kaushik Mitra et al. In: *Phys. Rev. B* 77 (21 2008), p. 214512. DOI: 10.1103/PhysRevB.77.214512.

[5] O. Buisson et al. In: *Quantum Information Processing* 8 (2-3 June 2009). DOI: 10.1007/s11128-009-0094-0.

[6] S. Lenz J et al.; Edelstein. In: *IEEE Sensors Journal* 6 (3 2006). DOI: 10.1109/jsen.2006.874493.

[7] Likharev. 1st ed. Gordon and Breach Science Publishers, 1986. ISBN: 2881240429,9782881240423.

[8] John M. Martinis. In: *Quantum Information Processing* 8 (2-3 June 2009). DOI: 10.1007/s11128-009-0105-1.